

Evaluating a Novel Approach of Finite Volume Method for Discretization of Seepage Equation in Embankment Dams, Case study: Sonbolerood dam

Hamid Reza Vosoughifar¹, Kamyar Mirabi¹, Armin Jalalzadeh²

1. Department of Civil Engineering, South Tehran Branch, Islamic Azad University, Tehran, Iran
2. Department of Civil Engineering, Ardabil Branch, Islamic Azad University, Ardabil, Iran

*Correspondence author: armin.jalalzadeh@gmail.com

Received: 10 July 2018/ **Accepted:** 30 September 2018/ **Published:** 30 September 2018

Abstract: This paper was concerned to simulate seepage phenomena (problems) via a novel approach. A high-resolution finite volume method (FVM) was employed to solve the two-dimensional (2D) seepage equations (SEs) using an unstructured grids. Voronoi mesh generation method has been exploited for grid generation method due to its special advantages. In this attempt, to reach to a proper accuracy, solving method obtained on even-odd steps was applied. The model named V-Seep (with MATLAB software) was run under different seepage conditions and then verified by comparing the model outputs with results obtained from different models and measured seepage. The Phase2-2D and Seep-W software which are based on FEM and a code based on FVM with triangular grids. Due to a precise agreement between those output and other software results, the V-Seep could be considered as a reliable method for dealing with seepage problems, especially in embankment dams. In addition, statistical observations indicated a good conformity between the V-Seep and measured data from a case study. The results indicated a higher efficiency and precision of the discrete equations resulted from the Voronoi mesh. Thus, it could be recommended to utilize the Voronoi mesh in the numerical discrete equations.

Keywords: Seepage, Embankment dam, Finite volume method, unstructured mesh, Voronoi mesh

1. Introduction:

Seepage through dam body and its foundations could redounded to dam failure and floods induced by dam failures can cause significant loss of human life and property damages, especially when located in highly populated regions. These entail numerical and laboratory investigations of seepage and their potential damage. In this approach the diffusion (Laplace's equation) equations (DEs) are conventionally used to describe the seepage flow. Many researchers studied the seepage in porous media and seepage flow through dam body and its foundation, such as Caffrey and Bruch Jr [1], Desai et al. [2], Gupta and Bruch

[3], Van Walsum and Koopmans [4], Chen et al.[5], Jianhong Zhang et al.[6], Guangxin et al.[7], Yuxin et al. [8], Bonelli [9], Jun-feng and Sheng [10], Shou-yi et al [11], Mohamed Abd El-Razek et al.[12], Tang Jing and Yongbiao [13], Kacimov and Obnosov [14], Navas and López [15], Rafiezadeh and Ashtiani [16], especially using numerical methods. Recently: H. Zheng et al.[17] introduced a new variational inequality formulation for seepage problems with free surfaces, in which a boundary condition of Signorini's type were prescribed over the potential seepage surfaces. They presented that via this formula the singularity of seepage points eliminated and the location of seepage points determined easily. Compared to



other variational formulations, the proposed formulation can effectively overcome the mesh dependency and significantly improve the numerical stability. JIANG Qing-hui et al. [18] proposed Three-dimensional numerical manifold approach for the unconfined seepage analysis and the tetrahedral finite element meshes were chosen as the mathematical meshes covering the whole volume. They developed an object-oriented program named 3DS-NMM and then applied it for seepage analysis of a homogenous earth dam. Hashemi Nezhad et al. [19] investigated the effect of solution arrangement of the grids (SAG) on accuracy of diffusion equation's solution and exploited MATLAB software for writing a code for solving algebraic equation set by using Line-by-line (LBL) solution method with alternative SAG. Kazemzadeh-Parsi and Daneshmand [20] introduced a three dimensional smoothed -fixed grid -finite element for evaluating unconfined seepage problems in inhomogeneous and anisotropic domains with arbitrary geometry to aim of facilitate solution of variable domain problems and improve the accuracy of the formulation of the boundary intersecting elements. Hasani et al. [21] evaluated amount of Seepage flow in earth fills dams (Ilam dams as a case study) using numerical models (Seep/W) with unstructured mesh, and then used the Slope/W software to evaluated the slope stability under different conditions. Yu-xin Jie et al. [22] used, the natural element method (NEM) as kind of meshless methods in the order to seepage analysis with free surface in dams via finite element method. NEM constructs shape functions based on the Voronoi diagrams. They introduced that NEM needs only the nodes information, and the pre-processing is simple. Since the nodes can be changed freely, the method is more suitable for dealing with problems that have changeable boundaries or boundaries dependent on computation results. Abhilasha et al. [23] presented the application of mathematical modeling of seepage in embankment dams and used Various software in the analysis of embankment dams like MODFLOW, SEEP/W, ANSYS, PLAXIS, PDEase2D, SVFLUX, etc., and were discussed them with reported case studies. Rafiezadeh and Ataie-Ashtiani [24] developed a boundary element method (BEM) for solving transient free-surface seepage problems in an anisotropic domain via finite difference method and evaluated the advantages of this approach with applied it for different cases. Later on Zheng et al. [25] presented the Primal mixed solution to unconfined seepage flow in porous media with

numerical manifold method and showed that their proposed procedure is able to accommodate complicated dam configuration and strong non-homogeneity. In recent year, Shahrokhbabadi et al. [26] presented an innovative boundary-type mesh-free method to determine the phreatic line location in unconfined seepage problems. Their method was developed based upon integrating the Method of Fundamental Solutions (MFS), Particle Swarm Optimization (PSO) algorithm, and Thiele Continued Fractions (TCF). To accurately estimate the phreatic line location, their proposed framework used MFS to solve the flow continuity equation, TCF to generate the phreatic line and PSO to optimize the phreatic line location generated by TCF. An excellent agreement was demonstrated upon comparison of their proposed method to the results attained from the analytical solutions and experimental tests. Finally Fukuchi [27] introduced a new method called interpolation finite difference method (IFDM) for solving two and three dimensional elliptic partial differential equations (PDEs) over complex domain and applied that for calculation of steady state seepage problem in unconfined domain. Compared results showed that the proposed method has adequate accuracy and wide applicability as a general method of numerically solving seepage problems. This paper attempts to present a novel development 2D seepage flow problems in homogeneous and in-homogenous media. A high-resolution FVM is employed to solve the diffusion equation on unstructured Voronoi mesh. The local Lax-Friedrichs (LLxF) scheme is used for the estimation of fluxes at cells and the numerical approximation of hyperbolic conservation laws. Table (1) is showing the general summarization of recent researches on numerical seepage analyses.

1-1 Research methodology

1-1-1 Governing Equations:

The general governing equations of seepage including the terms of convection and diffusion can be written in different forms depending upon the requirements of the numerical solution. The 2D form of it is introduced as follows:

$$\frac{\partial U}{\partial t} + \frac{\partial F}{\partial x} + \frac{\partial G}{\partial y} = S \quad (1)$$

$$U = \rho\phi \quad (2)$$

$$F = \rho u\phi - \Gamma \frac{\partial \phi}{\partial x} \quad (3)$$

$$G = \rho v\phi - \Gamma \frac{\partial \phi}{\partial y} \quad (4)$$

The parameter ϕ which could be quantities such as head, heat, mass, etc. and parameter Γ is the diffusion coefficient, u and v are the velocity and S is the source term. Flow in porous media like as some other phenomena such as heat, mass, potential flow, etc. could be studied via diffusion term of general governing equation.

1-1-2 Voronoi Mesh Generating Method:

Follows the German mathematician Johann Peter Gustav Lejeune Dirichlet (1850) who introduced the unstructured grid, Voronoi grids were further generalised by the Russian mathematician Georgy Feodosevich Voronoy (1908). Voronoi diagrams have been named after the latter author in computer science, while they were named Dirichlet tessellations in mathematics. During the last decades The Voronoi tessellation (grids) have been widely used in large number of fields in science and technology, even in art, and they have found numerous practical and theoretical applications. The contribution of Voronoi diagram to computer aided design, mathematic and engineering (CAD/CAM/CAE) has also been significant as it is one of major computational tools for geometric modeling, geometric processing, mesh generation and so on. Too many researches could be named which have used voronoi diagram in recent year, such as:

Wang et al. [28] proposed an adaptive crystal-growth Voronoi method to improve the representation of spatially continuous socioeconomic context in service area delimitation. They evaluated the continuous socioeconomic contexts (e.g., population distribution) and the compactness criterion (minimize travel time based on road network and natural barriers). Their proposed method innovatively distributed socioeconomic attributes using additional weighted raster planes and adaptively adjusted the crystal-growth speed based on real-time statistical results of the weights of each grown area. Geiß et al. [29] solved a transportation problem using Voronoi diagrams. They had given a geometric proof for the fact that additively weighted Voronoi diagram can optimally solve some cases of the Monge-Kantrovich transportation problem, where one measure has finite support, Wei Tu et.al. [30] proposed a bi-level Voronoi diagram metaheuristic to solve the large-scale multi-depot vehicle routing problem (MDVRP). Their computational experiments indicated that

the proposed metaheuristic can solve large-scale real-world MDVRPs more efficiently than many other state-of-the-art algorithms. Moreover, the proposed algorithm performs well with several small and medium-scale bench mark MDVRP instances, Jun Liu et al. [31] used Voronoi diagram algorithm for design and optimization bench blasting in open pit mines. They developed a code for the bench blast design in C++ and showed that their proposed method can greatly reduce the amount of the design work and validly improve the blast results, Pellerin et al. [32] proposed an automatic surface remeshing of 3D structural models based on Voronoi diagram. The main perspective of their method was to adapt it to volumetric meshing and used the generated meshes to solving partial differential equations describing coupled physical processes in the subsurface, Yongding Zhu and Jinhui Xu [33] Improved an algorithms for the farthest colored Voronoi diagram of line segments in the plane and achieved a tight upper bound on the combinatorial complexity of the farthest-color Voronoi diagram of n line segments with k different colors, Didandeh et al. [34] used the Voronoi diagrams to solve a hybrid facility location problem. They presented a solutions to located a set of facilities on a two dimensional space, with respect to a set of dynamic demand. Later on Dong-Ming et al. [35] presented an efficient algorithm to compute the clipped Voronoi diagram for a set of sites with respect to a compact 2D region or a 3D volume. Also they applied the proposed method to optimal mesh generation based on the centroidal Voronoi tessellation. At last El Said et al. [36] proposed a multi-scale modeling approach based on a 3D spatial Voronoi tessellation for predicting the mechanical behavior of 3D composites with accurate representation of the yarn architecture within structural scale models.

Basically, In the Voronoi mesh, the chosen point has lower distance in the devoted domain rather than other points. If one point has the same distance from several domains, it will be divided between domains. Indeed, these points create Voronoi cell boundaries. Consequently, internal sections of the Voronoi mesh consist of nodes belonging to one domain and boundaries include nodes that belong to several domains [37].

1-1-3 Numerical Modeling Algorithm:

The main advantage of the finite volume method (FVM) is that volume integrals in a partial differential Equation (PDE) containing a

divergence term are converted to surface integrals using the divergence theorem. These terms are then evaluated as fluxes at the surfaces of each FV.

Because the flux entering a given volume is identical to that leaving the adjacent volume, these methods are conservative. Another advantage of the FVM is that it is easily formulated to allow for unstructured meshes. Unstructured grid methods utilize an arbitrary collection of elements to fill the domain. These types of grids typically utilize triangles in 2D and tetrahedral in 3D, although quadrilateral, hexahedral, Voronoi, and Delaunay meshes can also be unstructured.

In this paper, the studied domain was discretized using unstructured Voronoi meshes. Delaunay triangulation was created and then the Voronoi mesh was established using the Qhull program in MATLAB software. The governing equation was discretized applying the FVM. In this approach, the studied domain was divided into several separated control volumes without any overlapping.

By integrating the governing differential equation over every control volume, the system of algebraic equations was created so that each of its formulations belonged to one control volume and each equation linked a parameter in the control volume node to different numbers of the parameter in adjacent nodes. This consequently led to the computation of the parameter in each node [38].

In order to solve discrete equations, the parameter in each node was computed considering its discrete equation and newest adjacent nodes' values. Solution procedure can be expressed as follows.

- (1) Assuming an initial value in each node as an initial condition.
- (2) Calculating the value in a node considering its discrete equation.
- (3) Performing pervious step for all nodes over the studied domain, one cycle is performed by repetition this step.
- (4) Verifying the convergence clause. If this clause is satisfied, the computing will end otherwise the computations will be repeated from the second step.

As exact values of boundary conditions were not distinct, the Riemann boundary condition was utilized for computing the investigating parameter. Therefore, by assuming a layer

which is close to the boundary layer, $\partial/\partial x=0$ and $\partial/\partial y=0$ were defined for the investigating parameter and then, calculated values for boundary adjacent nodes transform to related boundary nodes. This procedure will continue until the results difference is converged.

1-1-4 Discretization of Governing Equations:

1-1-4-1 FV Discretization:

Various methods can be used to discretize the governing equations, among which the FVM due to its ability to satisfy mass and momentum conservation is frequently adopted. In this research, the discretization of equation (1) was performed using the FVM with unstructured Voronoi mesh, as shown in Fig.1.

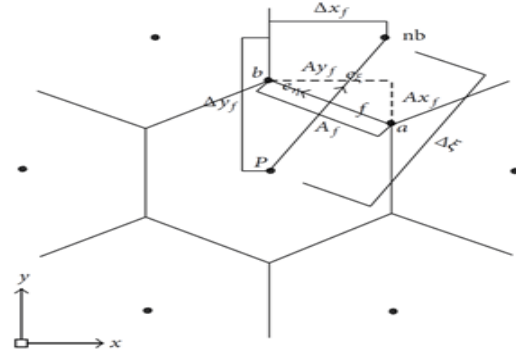


Fig.1. The 2D schematic Voronoi mesh cell used for describing the discretization of the governing equations

The 1st steps discretization process with Voronoi mesh is given by equation (5) and equation (6).

$$\iint_A \frac{\partial u}{\partial t} dA + \iint_A (\vec{\nabla} \cdot \vec{n}) dl = \iint_A S dA \quad (5)$$

By implementing divergence theorem, equation (5) is yielded to equation (6) as follows:

$$\iint_A \frac{\partial U}{\partial t} dA + \oint_l (\vec{H} \cdot \vec{n}) dl = \iint_A S dA \quad (6)$$

Where $\vec{H} = \vec{F}_i + \vec{G}_j$ Equation (6) can be written as equation (7) by approximating the line integral for all control volumes and nodes, generally,

$$\frac{dU_i}{dt} = -\frac{1}{A_i} \sum_j (\vec{H} \cdot \vec{n}_{ij} \Delta l_{ij}) + S_i \quad (7)$$

1-1-4-2 FV Discretization:

By applying the Voronoi mesh, equation (7) is yielded to equation (8) for an investigated control volume; however, Figure 1 illustrates the 2D Voronoi mesh grid used for describing these equations as follows:

$$\frac{\partial U}{\partial t} = -\frac{1}{A} \sum_f (\vec{H} \cdot A \vec{e}_\varepsilon)_f + S \quad (8)$$

$$\vec{H} = H_\varepsilon \cdot \vec{e}_\varepsilon + H_\eta \cdot \vec{e}_\eta \quad (9)$$

$$\frac{\partial U}{\partial t} = -\frac{1}{A} \sum_f H_f A_f + S \quad (10)$$

$$\int_t^{t+\Delta t} \frac{\partial U}{\partial t} dt = \int_t^{t+\Delta t} \left(-\frac{1}{A} \sum_f H_\varepsilon A_f \right) dt + \int_t^{t+\Delta t} S dt \quad (11)$$

$$U_p^{n+1} - U_p^n = -\frac{1}{A} \sum_f H_\varepsilon A_f \Delta t + S \Delta t \quad (12)$$

$$H_\varepsilon = n_1 F_\varepsilon + n_2 G_\varepsilon \quad (13)$$

$$n_1 = \frac{(x_{nb} - x_p)}{\sqrt{(x_{nb} - x_p)^2 + (y_{nb} - y_p)^2}} \quad (14)$$

$$n_2 = \frac{(y_{nb} - y_p)}{\sqrt{(x_{nb} - x_p)^2 + (y_{nb} - y_p)^2}} \quad (15)$$

The discrete equation can be written as equation (16),

$$U_p^{n+1} = U_p^n - \frac{\Delta t}{A} \sum_f [n_1 F_\varepsilon A_f + n_2 G_\varepsilon A_f]^n + S^n \Delta t \quad (16)$$

1-2 The Local Lax-Friedrichs (LLxF) High-Order Scheme.

In shock capturing schemes, the location of discontinuity is captured automatically by the scheme as a part of the solution procedure. These slope-limiter or flux-limiter methods can be extended to systems of equations. In this paper, the algorithm is based on hybrid differences with comparable performance to Riemann type solvers used to obtain a solution for PDE's describing systems. Finite Volume (FV) and Finite Difference (FD) methods are closely related to central schemes like the most shock capturing schemes [39]. Rusanov scheme is often called the LLxF method, because it has the same form as the Lax-Friedrichs (LxF) method but the lateral diffusion is chosen locally. It means that it is less diffusive than normal LxF, since it locally limits the numerical lateral diffusion instead of having a uniform lateral diffusion on the entire domain.

Many researchers (e.g., Lin et al. [40], van Dam and Zegeling [41], and Lu et al. [42]) utilized

LLxF splitting scheme in different problems such as 2D SWEs, 1D adaptive moving mesh method and its application to hyperbolic conservation laws from magneto hydrodynamics (MHD), and the performance of the weighted essential non oscillatory (WENO) method.

In this research, LLxF is used as a flux calculator. By expanding equations (16), equation (17) can be written as follows:

$$U_p^{n+1} = U_p^n - \frac{\Delta t}{A} \left[\sum_f \left((F_f)_{nb.out} A_f n_{1f} \right) + \sum_f \left((F_f)_{nb.in} A_f n_{1f} \right) + \sum_f \left((G_f)_{nb.out} A_f n_{2f} \right) - \sum_f \left((G_f)_{nb.in} A_f n_{2f} \right) \right] + S \Delta t \quad (17)$$

The parameters in equation (1) to (4) for seepage flow via Laplace's equation described as below:

$$\varphi = h \quad \& \quad \Gamma = k \quad (18)$$

$$F = u = \Gamma \frac{\partial \varphi}{\partial x} \quad (19)$$

$$G = v = \Gamma \frac{\partial \varphi}{\partial y} \quad (20)$$

$$U = h \text{ and } S = 0 \quad (21)$$

Inter-cell fluxes can be estimated by implementing the following equations:

$$(F_f)_{nb.out} = \frac{F(u_{nb}^n) + F(u_p^n)}{2} \quad (22)$$

$$(F_f)_{nb.in} = \frac{F(u_{nb}^n) + F(u_p^n)}{2} \quad (23)$$

$$(G_f)_{nb.out} = \frac{G(v_{nb}^n) + G(v_p^n)}{2} \quad (24)$$

$$(G_f)_{nb.in} = \frac{G(v_{nb}^n) + G(v_p^n)}{2} \quad (25)$$

After computing inter-cell fluxes by utilizing the LLxF scheme in Voronoi mesh, equations can be solved and the final result can be calculated for each time step. The Δt can be computed using the Courant Friedrichs-Lewy (CFL) for each time step as follows:

The CFL should be range over [0,1] for

achieving to the stability ($0 < CFL < 1$).

$$\Delta t = CFL \times \min \left(\sqrt{(x_{nb} + x_p)^2 + (y_{nb} + y_p)^2} \right) \quad (26)$$

Table 1. General Summarization of methods and software used by some other studies

References	Hasani	Kazemzade	Yu-xin	Abhilasha	Jiang	Rafiezade	This article
Numerical Method	FEM	FEM	NEM	FEM	NMM	FDM	FVM
Applied Software	Com. Soft.	3D SFGFEM	Seepdam	Com. Soft.	3DS NMM	SEEPBEM3D	V-Seep
Mesh Grid	Unstructured Grids	NBFM	Mesh-less	Various	Tetrahedral FE Mesh	BEM	Unstructured Voronoi
Dimensional approach	2D	3D	2D	2D,3D	3D	3D	2D
Studied Field	Earth fill Dam	Unconfined seepage Flow	Free Surface Seepage in Dams	Earth fill Dam	Earth fill Dam	Earth fill Dam and well	Earth fill Dam

1-3 Preparation and Validation of the Numerical Algorithm

The CFD code named V-Seep was prepared on the novel approach of unstructured Voronoi grid. V-Seep was then validated using real measured data from a case study. In mentioned program, after creating the case geometry, the Voronoi mesh algorithm is generated the proper meshes for described domain. With introducing the boundary layers and material properties, analyzing process was started. V-Seep is produced to calculating the seepage flow through the embankment dams. Due to this aim the geometry of an embankment dam is introduced to V-Seep program and then with using of correlation method for producing the upper stream-line flow in dam body (Phreatic line), the piezometric head and flow discharge in all nodes was calculated. The potential line and stream-line in dam body is plotting accordingly.

The case study which has been used in this research is the right embankment zone of Sonboleroud dam placed in north part of Iran cross the branch of Babol River. The mentioned zone of the dam has a length of about 30 m which stands adjacent to the dam spillway

walls. The upstream slope of the dam which is contact with water is 1:3.3 and downstream part slope is 1:1.9. Embankment width in top is 1 m and in bottom which connecting to foundation is 18.5m. During the flood events water raise up to 1.8 m above upstream face of embankment dam. Hydraulic conductivity based on geo-technique analysis is 3.44E-05 m/s. Boundary condition that is considered for this case study contained the pervious and impervious boundary and water level up/downstream of the embankment. Nodes initial values for different volume is gaining from using of specified nodes piezometric head values attribution. Mentioned values is described via up/downstream potential lines and applied in boundary conditions. Figs.2 to 4 show the case study satellite view and geometry.

In present article for verification and certainty of precision of produced program, different testes such as static, dynamic and stability tests were done. Then the obtained results were compared with real measured data from the case study. Fig.5 shows the Voronoi mesh generation for presented geometry.



Fig.2. Sonboleroud dam satellite view

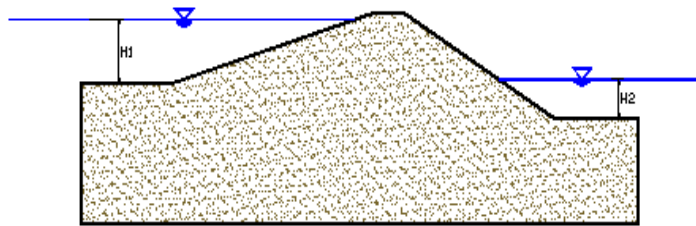


Fig.4. Case Study Geometry

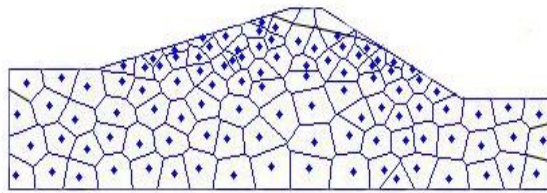


Fig.5.Voronoi Mesh Generation for studied Case

One of the important tests for verification of the program is the model sensibility to usage of different mesh generation method. Due to this fact the prescribed geometry is meshing with regular rectangular-triangular meshes and the novel approach of V-Seep model. Output result compared with obtained result from Voronoi unstructured grids method. Figs.6 to 9 and table (2) show the mesh generation and output result for various mesh generation methods. Existing of trivial variance between two mentioned results, indicted Voronoi grid technique is proper approach for mesh generation in complex geometry with certainty. The seepage rate has been measured for described studied zone is about $3.74E-05$ m³/sec/m.

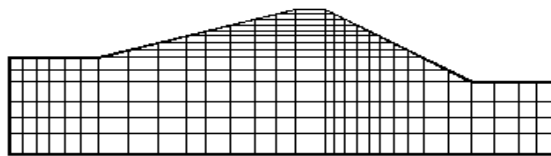


Fig.6.Rectangular- Triangular Mesh

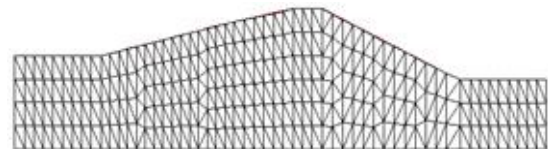


Fig.7.Triangular Mesh

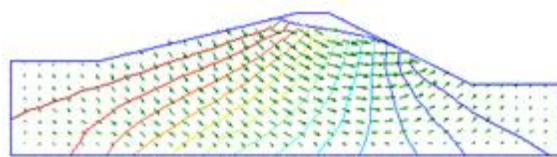


Fig.8.Potential Line and Net Flow (Rec. Tri. Mesh)

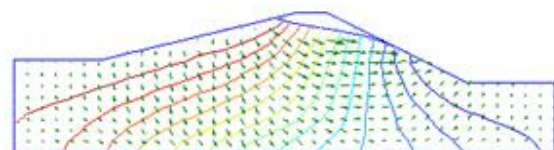


Fig.9.Potential Line and Net Flow (Voronoi Mesh)

Table2. Seepage values for various mesh generation methods

Mesh Generation Method	FVM with Triangular Mesh	FVM with Rectangular-Triangular Mesh	FVM With Voronoi Unstructured Mesh
Calculated Discharge m ³ /sec/m	3.78E-05	3.89E-05	3.66E-05

In researches and studies obtained on computational approach, time is the most important parameter. Reaching to accurate result in majority of numerical method based on small grid dimensions and increasing the number of calculation equation and consuming the time accordingly. Due to mentioned fact the V-Seep program tests with 3 different mesh size. The results show that the presented method has low sensibility to mesh size and is suitable for big domain. Fig.10 show the small size Voronoi mesh generation and table (3) show the V-Seep program output results using different Voronoi mesh generation size.

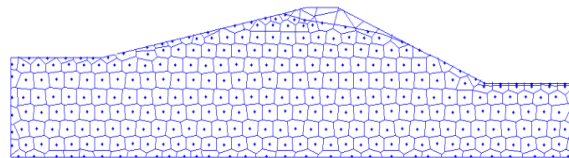


Fig.10. Small Size Voronoi Mesh Generation

Table3. Seepage values for different Voronoi mesh size

Mesh Size	V-Seep with Small Mesh Size	V-Seep with Medium Mesh Size	V-Seep with Large Mesh Size
Calculated Discharge m ³ /sec/m	3.66E-05	3.73E-05	3.85E-05

2- Discussion and conclusion

After validation process of V-Seep program the case study is evaluated via common software for seepage analyzing such as Seep/W and Phase2-2D. Figs.12 to 15 show the mesh generation and output results with Seep/W and Phase2 software. Table (4) shows the comparison between calculated seepage quantities from various methods.

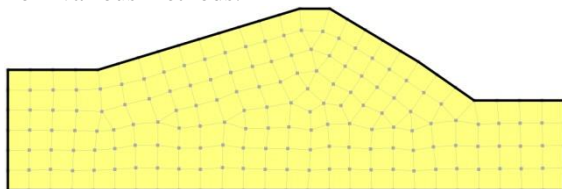


Fig.11. Seep/W Mesh Generation

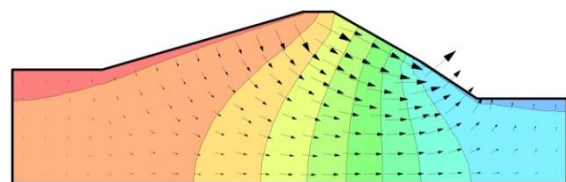


Fig.12. Potential Line and Net Flow (Seep/W Output)

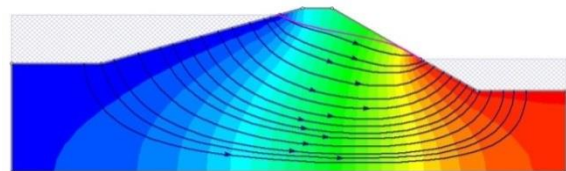
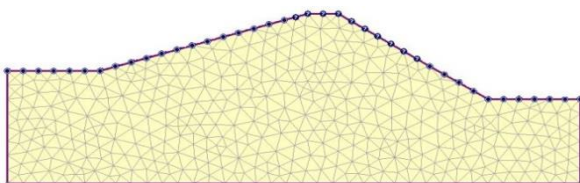


Fig.13.Phase2 Mesh Generation

Fig.14.Potential Line and Net Flow (Phase2 Output)

Table4.Seepage values from various models

Used Software	V-Seep	Seep/W	Phase2-2D
Calculated Discharge m3/sec/m	3.66E-05	3.83E-05	3.54E-05

Fig.15 and 16 show the phreatic line diagram from different calculated methods and measured data.

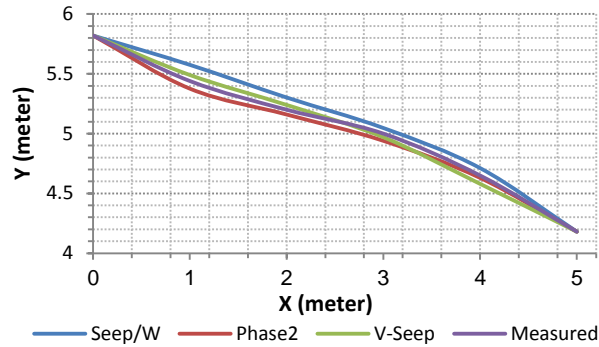


Fig.15. Phreatic Line Diagram

For evaluation of calculated results the Mann-Whitney test has been used and the results show no significant differences between calculated results via V-Seep model and the real measured data (P.Value=.99). Also P-value for Seep/W and Phase2 models showed proper accuracy with real measured data. Fig.17 and table (4) show the results of the Mann-Whitney test for statistical analyses between the obtained results using V-Seep and other models.

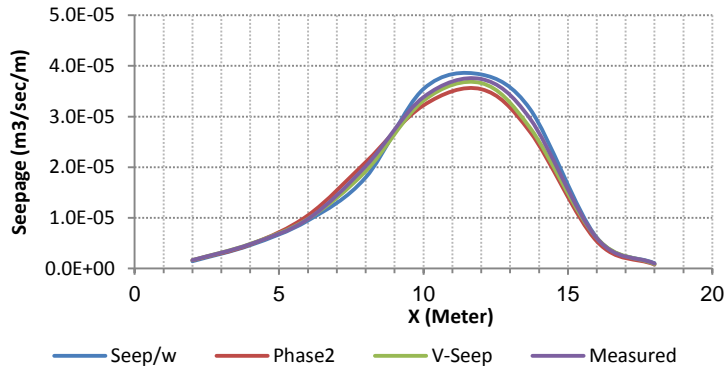


Fig.16. Seepage along x axis

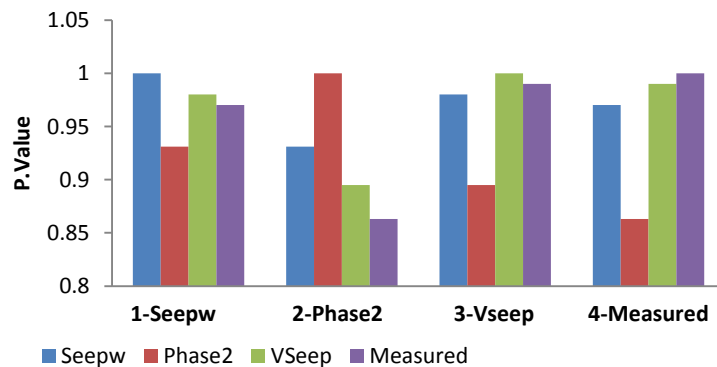


Fig.17. Comparison between V-Seep results and other models

Table4. Mann-Whitney test parameters for comparison between V-Seep and other models and measured data.

Output result	Parameter			
	Mann-Whitney U	Wilcoxon W	Z	P value
Seep /W	39.60	84.50	-0.039	0.981
Phase2	39.00	84.00	-0.132	0.931
Measured data	40.00	85.00	-0.044	0.991

In the current research, a novel and friendly user code named V-Seep was evaluated. This novel code was showing that the LLxF scheme along with the FVM on the unstructured Voronoi grid is a suitable combination in order to simulate 2D Seepage problems. The advantages of this method are very promising, especially in reconstructing the conducted tests. For 2D seepage flow, real measured data was considered for validation. Obtained results demonstrated that there are no significant differences between real measured results and V-Seep outputs. In addition obtained Results were compared with some other common software in seepage analyzing such as Seep/w (Geo-slope Co.) and Phase2-2D (Rocscience Co.) and no significant numerical dispersion problem or nonphysical alternation was observed in the results. The comparison showed a good agreement between V-Seep results with mentioned software. In terms of mesh grid comparison, it was seen that the Voronoi mesh grid results are closer to triangular mesh grid results. In addition generally the unstructured Voronoi mesh grid is able to model inlet and outlet fluxes in every direction of control volume faces. Node values impressibility proportional to assigned area from adjacent nodes, leads to creating more uniform condition of diffusion and pressure distribution in studied area. Also due to low interacts of output results gained from V-Seep program by mesh size, the presented method (FVM-Voronoi mesh) shall be a recommended choice instead of previous method such as FEM. The results indicated a

higher efficiency and precision of the discrete equations resulted from the Voronoi mesh. Thus, it could be recommended to utilize the Voronoi mesh in the numerical discrete equations. The Voronoi mesh grid is able to model complicated geometries, and also it could produce the final discrete equations leading to accurate results within a lower computational demand compared to other unstructured meshes.

Nomenclatures

- A: Area of the adjacent surface vector of the investigated Voronoi cell (\vec{A})
- A_x : The component of A in x direction
- A_y : The component of A in y direction
- F,G: Flux vector functions
- F_e, G_e : The Voronoi cell normal flux vectors
- U: The vector of conserved variables
- H: Input and output fluxes to a Voronoi cell
- S: The vector of source terms
- S_{0x} : Bed slope in the x direction
- S_{0y} : Bed slope in the y direction
- a,b: Nodes of the both sides of the investigated Voronoi cell f
- e_ξ : Unit outward normal vector in each Voronoi cell f
- e_η : The unit tangent vector in each Voronoi cell f
- \vec{f} : Joint surface element between investigated cell and other adjacent cells
- \vec{g} : Gravity acceleration
- h: The water depth
- \bar{h} : The mean water depth
- h_u : The upstream water depth at $t = 0$
- h_d : The downstream water depth at $t = 0$
- l: The boundary of the i th control volume
- n: The Manning's roughness coefficient
- \vec{n} : The outward unit vector normal to the boundary
- nb: The central node of adjacent cells
- t: Time

- u : Velocity vector component in x direction
 \bar{u} : The mean velocity vector component in x direction
 v : Velocity vector component in y direction
 \bar{v} : The mean velocity vector component in y direction
 x : Horizontal coordinate component
 y : Vertical coordinate component
 $\sum f$: The sum over the all Voronoi cells
 p : Central node of investigated Voronoi cell
 Δt : Time interval
- Out:**
 Denotes the parameter outside the Voronoi cells side's area f
 ξ : The parameter component in $e\xi$ direction
 η : The parameter component in $e\eta$ direction
Superscripts:
 $\Delta\xi$: The distance between the central node of investigated Voronoi cell
- H_0 : The null hypothesis
 Z : The value of Z-Test
 Z_0 : The critical value of Z extracted from the statistical Z-distribution graph
 $RS1$: Sum of ranks for the first comparing group
 $RS2$: Sum of ranks for the second comparing group
 α : The significance level
 N_A : The number of data in the first comparing group
 N_B : The number of data in the second comparing group
- Subscripts:**
 f : Denotes the parameter at the Voronoi cells side's area f
 i : Counts all central control volumes
 j : Counts all nodes of the central control volumes
 nb : Denotes parameters at the central node of adjacent Voronoi cells
 p : Denotes parameters at central node of investigated Voronoi cell
 in :
 Denotes the parameter outside the Voronoi cells side's area f
 n : Denotes parameters belonging to time of t
 $n+1$: Denotes parameters belonging to time of $t + \Delta t$

References

- [1] John Caffrey, John C Bruch Jr., Three-dimensional seepage through a homogeneous dam, *Advances in Water Resources*, Volume 2, March 1979, Pages 167-176
- [2] C.S. Desai, J.G. Lightner, S. Somasundaram, A numerical procedure for three-dimensional transient free surface seepage, *Advances in Water Resources*, Volume 6, Issue 3, September 1983, Pages 175-181
- [3] C.S.Gupta, J.C. Bruchjr, V.Comincioli, Three dimensional unsteady seepage through an earth dam with accretion, *Engineering Computations* Vol.3, issue 1, March 1986, P2-10
- [4] P.E.V Van Walsum, R.W.R Koopmans, Steady two-dimensional groundwater seepage-numerical analysis in the $\phi\psi$ -plane, *Journal of Hydrology*, Volume 72, Issues 3-4, 15 June 1984, Pages 331-354
- [5] J.T.Chen, H.-K. Hong, S.W. Chyuan, Boundary element analysis and design in seepage problems using dual integral formulation, *Finite Elements in Analysis and Design*, Volume 17, Issue 1, June 1994, Pages 1-20
- [6] Jianhong Zhang, Qianjun Xu, Zuyu Chen, Seepage analysis based on the unified unsaturated soil theory, *Mechanics Research Communications*, Volume 28, Issue 1, January-February 2001, Pages 107-112
- [7] Guangxin Li, Jinhong Ge, Yuxin Jie, Free surface seepage analysis based on the element-free method, *Mechanics Research Communications*, Volume 30, Issue 1, January-February 2003, Pages 9-19
- [8] Yuxin Jie, Guanzhou Jie, Zeyu Mao, Guangxin Li, Seepage analysis based on boundary-fitted coordinate transformation method, *Computers and Geotechnics*, Volume 31, Issue 4, June 2004, Pages 279-283
- [9] Stéphane Bonelli, Approximate solution to the diffusion equation and its application to seepage-related problems, *Applied Mathematical Modelling*, Volume 33, Issue 1, January 2009, Pages 110-126
- [10] Jun-feng FU, Sheng JIN, A study on unsteady seepage flow through dam, *Journal of*

- Hydrodynamics, Ser. B, Volume 21, Issue 4, August 2009, Pages 499-504
- [11] Shou-yi Li, Yan-long Li, Zheng Si, Xiao-fei Zhang, A seepage computational model of face slab cracks based on equi-width joint constant flow, *Advances in Engineering Software*, Volume 41, Issues 7–8, July–August 2010, Pages 1000-1004
- [12] Mohamed Abd El-Razek M. Rezk, Abd El-Aziz Ahmed Ali Senoon, Analytical solution of seepage through earth dam with an internal core, *Alexandria Engineering Journal*, Volume 50, Issue 1, March 2011, Pages 111-115
- [13] Tang Jing, Liu Yongbiao, Penalty Function Element Free Method to Solve Complex Seepage Field of Earth Fill Dam, *IERI Procedia*, Volume 1, 2012, Pages 117-123
- [14] Anvar Kacimov, Yurii Obnosov, Analytical solutions for seepage near material boundaries in dam cores- The Davison–Kalinin problems revisited, *Applied Mathematical Modelling*, Volume 36, Issue 3, March 2012, Pages 1286-1301
- [15] Pedro Navas, Susana López-Querol, Generalized unconfined seepage flow model using displacement based formulation, *Engineering Geology*, Volume 166, 8 November 2013, Pages 140-151
- [16] K. Rafiezadeh, B. Ataie-Ashtiani, Seepage analysis in multi-domain general anisotropic media by three-dimensional boundary elements, *Engineering Analysis with Boundary Elements*, Volume 37, Issue 3, March 2013, Pages 527-541
- [17] H. Zheng, D.F. Liu, C.F. Lee and L.G. Tham, A new formulation of Signorini’s type for seepage problems with free surfaces, *International Journal for Numerical Methods in Engineering*, Volume 64, Issue 1, 07 September 2005 pages 1–16.
- [18] Jiang Qing-hui, Deng Shu-shen, Zhou Chuang-bing, Lu Wen-bo, Modeling Unconfined Seepage Flow Using Three Dimensional Numerical Manifold Method, *Journal of Hydrodynamic*, Volume 22, Issue 4, 01 August 2010, Pages 554-561
- [19] S. Reza Hashemi Nezhad and Hamid Reza Vosoughifar, Solution Arrangement Effect on Line-by-Line Method’s Accuracy in Analysis of dam’s Foundation, *International Journal of Computational Methods*, Vol. 8, No. 3 (2011) 583–596
- [20] Mohammad Javad Kazemzadeh-Parsi, Farhang Daneshmand, Three dimensional smoothed fixed grid finite element method for the solution of unconfined seepage problems, *Finite Elements in Analysis and Design*, Volume 64, February 2013, Pages 24-35
- [21] H. Hasani, J. Mamizadeh and H. Karimi, Stability of Slope and Seepage Analysis in Earth Fills Dams Using Numerical Models (Case Study: Ilam DAM-Iran), *World Applied Sciences Journal*, Vol. 21 Issue 9, 2013, pages 1398-1402
- [22] Yu-xin Jie, Li-zhen Liu, Wen-jie Xu, Guang-xin Li, Application of NEM in seepage analysis with a free surface, *Mathematics and Computers in Simulation*, Volume 89, March 2013, Pages 23-37
- [23] Ms. Abhilasha P. S., T. G. Antony Balan, Numerical Analysis of Seepage in Embankment Dams, *IOSR Journal of Mechanical and Civil Engineering (IOSR-JMCE)(ICICE)*, vol.4, 2014, pages 13-23
- [24] K. Rafiezadeh, B. Ataie-Ashtiani, Transient free-surface seepage in three-dimensional general anisotropic media by BEM, *Engineering Analysis with Boundary Elements*, Volume 46, September 2014, Pages 51-66
- [25] Hong Zheng, Feng Liu, Chunguang Li, Primal mixed solution to unconfined seepage flow in porous media with numerical manifold method, *Applied Mathematical Modeling*, Volume 39, Issue 2, 15 January 2015, Pages 794-808
- [26] Shahriar Shahrokhhabadi, Farshid Vahedifard , Shantia Yarahmadian, Integration of Thiele Continued Fractions and the method of fundamental solutions for solving unconfined seepage problems, *Computers and Mathematics with Applications*, Volume 71, Issue 7, April 2016, Pages 1479-1490
- [27] Fukuchi , Numerical analyses of steady-state seepage problems using the interpolation finite difference method, *Soil and Foundation*, Volume 56, Issue 4, August 2016, Pages 608–626
- [28] Jue Wang, Mei-Po Kwan, LinBing Ma, Delimiting service area using adaptive crystal-growth Voronoi diagrams based on weighted planes:-A case study in Haizhu District of Guangzhou in China, *Applied Geography*, Volume 50, June 2014, Pages 108-119
- [29] Darius Geiß, Rolf Klein, Rainer Penninger, Günter Rote, Reprint of Optimally solving a transportation problem using Voronoi diagrams, *Computational Geometry*, Volume 47, Issue 3, Part B, April 2014, Pages 499-506
- [30] Wei Tu, Zhixiang Fang, Qingquan Li, Shih-Lung Shaw, BiYu Chen, A bi-level Voronoi

diagram-based metaheuristic for a large-scale multi-depot vehicle routing problem, *Transportation Research Part E, Logistics and Transportation Review*, Volume 61, January 2014, Pages 84-97

[31] Jun Liu, Pinyu Sun, Fangxue Liu, Mingsheng Zhao, Design and optimization for bench blast based on Voronoi diagram, *International Journal of Rock Mechanics and Mining Sciences*, Volume 66, February 2014, Pages 30-40

[32] Jeanne Pellerin, Bruno Lévy, Guillaume Caumon, Arnaud Botella, Automatic surface remeshing of 3D structural models at specified resolution - A method based on Voronoi diagrams, *Computers & Geosciences*, Volume 62, January 2014, Pages 103-116

[33] Yongding Zhu, Jinhui Xu, Improved algorithms for the farthest colored Voronoi diagram of segments, *Theoretical Computer Science*, Volume 497, 29 July 2013, Pages 20-30

[34] Arman Didandeh, Bahram Sadeghi Bigham, Mehdi Khosravian, Farshad Bakhshandegan Moghaddam, Using Voronoi diagrams to solve a hybrid facility location problem with attentive facilities, *Information Sciences*, Volume 234, 10 June 2013, Pages 203-216.

[35] Dong-Ming Yan, Wenping Wang, Bruno Lévy, Yang Liu, Efficient computation of clipped Voronoi diagram for mesh generation, *Computer-Aided Design*, Volume 45, Issue 4, April 2013, Pages 843-852

[36] Bassam El Said, Dmitry Ivanov, Andrew C. Long, Stephen R. Hallett, Multi-scale modelling of strongly heterogeneous 3D composite structures using spatial Voronoi tessellation, *Journal of the Mechanics and Physics of Solids*, Volume 88, March 2016, Pages 50-71.

[37] T. A. Prickett, Modeling techniques for groundwater evaluation, *Advances in Hydro science*, vol. 10, 1975, pp. 1-143.

[38] C. A. J. Fletcher, *Computational Techniques for Fluid Dynamics*, vol. 2, Springer, Berlin, Germany, 2nd edition, 1991.

[39] V. V. Rusanov, The calculation of the interaction of non stationary shock waves with barriers, *Journal of Computational and Mathematical Physics USSR*, vol. 1, 1961, pp. 267-279.

[40] G. F. Lin, J. S. Lai, and W. D. Guo, Finite-volume component wise TVD schemes for 2D shallow water equations, *Advances in Water Resources*, vol. 26, no. 8, 2003, pp. 861-873.

[41] A. van Dam and P. A. Zegeling, A robust moving mesh finite volume method applied to 1D hyperbolic conservation laws from magneto hydrodynamics, *Journal of Computational Physics*, vol. 216, no. 2, 2006, pp. 526-546.

[42] C. Lu, J. Qiu, and R. Wang, A numerical study for the performance of the WENO schemes based on different numerical fluxes for the shallow water equations, *Journal of Computational Mathematics*, vol. 28, no. 6, 2010, pp. 807-825.